

Controlled Hydrogen Peroxide Decomposition for a Solid Oxide Fuel Cell (SOFC) Oxidant Source with a Microreactor Model

E. Lennon¹, A. Burke², and R. Besser¹

¹ CBME Department: Stevens Institute of Technology, Hoboken, NJ 07030

² Naval Undersea Warfare Center, Newport, RI

Abstract: A microchannel reactor for hydrogen peroxide decomposition is being developed for integration with fuel cell systems that can power undersea vehicles. However, the catalytic decomposition of H_2O_2 is predisposed to thermal runaway. A micro-scale packed bed reactor (MPBR), theoretically capable of inhibiting thermal runaway, is under development in COMSOL to illustrate thermal management and oxygen production during this reaction. The COMSOL model solves mass, energy, and momentum balances to simulate temperature and concentration profiles within the reactor. Using a stainless steel block around the capillary to act as an extended surface for higher heat removal rates and an initial volumetric flow rate of $2\text{e}^{-9} \text{ m}^3/\text{s}$ (about 0.1 ml/min), a temperature rise less than 8 K was simulated and an outlet concentration of 1716 mol/m^3 oxygen was achieved. Overall the results indicate that thermally-controlled oxygen generation from hydrogen peroxide decomposition is feasible in a microreactor provided there is sufficient external surface area to facilitate convective cooling.

Keywords: Micro-reactor, Oxidant, Multiphase Modeling.

1. Introduction

A major challenge facing the design of air-independent power systems is continuous energy generation. High energy density and potentially low operating costs make fuel cell power systems an attractive option for high endurance, air-independent, undersea vehicle applications.¹ However air-independent fuel cell power systems require an oxidant supply. Hydrogen peroxide (H_2O_2) decomposes into water (H_2O) and oxygen (O_2) [$\text{H}_2\text{O}_2 \rightarrow \text{H}_2\text{O} + \frac{1}{2} \text{O}_2$] providing a dense source of oxygen per unit volume that makes it a valuable commodity as an air-independent fuel cell oxidant.

The high oxygen density (0.0215 O_2 moles/ml in 50% H_2O_2 liquid solution compared to 0.035 O_2 moles/ml in solid NaClO_3 for example)² ease of handling, and commercial infrastructure

of H_2O_2 add to its appeal as an oxidant source.³ Despite these advantages, it is well established that catalytic H_2O_2 decomposition is susceptible to thermal runaway, which has historically limited its application as a power system oxidant.⁴ Microchemical systems by virtue of microscale geometry (relevant fluid dimension in subunits $< 1 \text{ mm}$), possess high surface-to-volume ratios resulting in heat and mass transfer coefficients capable of inhibiting thermal runaway.⁵ Thus, microchemical systems present a theoretical mechanism to harness the aforementioned benefits of a hydrogen peroxide oxidant source, and at the same time prevent thermal runaway during the exothermic reaction.

The aim of this on-going modeling effort is to demonstrate oxygen production and thermal management feasibility during the catalytic multiphase decomposition of hydrogen peroxide in one of the subunits of a microchemical reactor system. The basis of the present model is a microchannel reactor. The model description, governing equations and assumptions, and boundary conditions follow in section two. Next, the simulation results illustrating temperature and concentration profiles are shown. Finally, a summary is given for the current model's capabilities and limitations and areas for future modification intended to better evaluate multiphase microscale flow effects on this reaction are identified.

2. Methods

2.1 Model Description

In order to simulate the catalytic multiphase decomposition of hydrogen peroxide in a microreactor, a channel of sub-millimeter radius (0.5 mm) containing catalyst was modeled (Figure 1). The cross sectional geometry of the reactor channel resembled a half moon. The channel proceeded straight down the length of the reactor (5cm). Surrounding the channel was a rectangular stainless steel 316 block (7x2x0.4 cm). To mimic upcoming experimental conditions, a Plexiglas (PMMA) cover (7x2x0.1 cm) served as the microreactor seal.

Report Documentation Page			Form Approved OMB No. 0704-0188		
Public reporting burden for the collection of information is estimated to average 1 hour per response, including the time for reviewing instructions, searching existing data sources, gathering and maintaining the data needed, and completing and reviewing the collection of information. Send comments regarding this burden estimate or any other aspect of this collection of information, including suggestions for reducing this burden, to Washington Headquarters Services, Directorate for Information Operations and Reports, 1215 Jefferson Davis Highway, Suite 1204, Arlington VA 22202-4302. Respondents should be aware that notwithstanding any other provision of law, no person shall be subject to a penalty for failing to comply with a collection of information if it does not display a currently valid OMB control number.					
1. REPORT DATE OCT 2007		2. REPORT TYPE		3. DATES COVERED 00-00-2007 to 00-00-2007	
4. TITLE AND SUBTITLE Controlled Hydrogen Peroxide Decomposition for a Solid Oxide Fuel Cell (SOFC) Oxidant Source with a Microreactor Model				5a. CONTRACT NUMBER	
				5b. GRANT NUMBER	
				5c. PROGRAM ELEMENT NUMBER	
6. AUTHOR(S)				5d. PROJECT NUMBER	
				5e. TASK NUMBER	
				5f. WORK UNIT NUMBER	
7. PERFORMING ORGANIZATION NAME(S) AND ADDRESS(ES) Stevens Institute of Technology, CBME Department, Hoboken, NJ, 07030				8. PERFORMING ORGANIZATION REPORT NUMBER	
9. SPONSORING/MONITORING AGENCY NAME(S) AND ADDRESS(ES)				10. SPONSOR/MONITOR'S ACRONYM(S)	
				11. SPONSOR/MONITOR'S REPORT NUMBER(S)	
12. DISTRIBUTION/AVAILABILITY STATEMENT Approved for public release; distribution unlimited					
13. SUPPLEMENTARY NOTES Presented at the 2007 COMSOL Users Conference Boston, 4-6 Oct, Newton. MA					
14. ABSTRACT A microchannel reactor for hydrogen peroxide decomposition is being developed for integration with fuel cell systems that can power undersea vehicles. However, the catalytic decomposition of H₂O₂ is predisposed to thermal runaway. A micro-scale packed bed reactor (MPBR), theoretically capable of inhibiting thermal runaway, is under development in COMSOL to illustrate thermal management and oxygen production during this reaction. The COMSOL model solves mass, energy, and momentum balances to simulate temperature and concentration profiles within the reactor. Using a stainless steel block around the capillary to act as an extended surface for higher heat removal rates and an initial volumetric flow rate of 2e-9 m³/s (about 0.1 ml/min), a temperature rise less than 8 K was simulated and an outlet concentration of 1716 mol/m³ oxygen was achieved. Overall the results indicate that thermally-controlled oxygen generation from hydrogen peroxide decomposition is feasible in a microreactor provided there is sufficient external surface area to facilitate convective cooling.					
15. SUBJECT TERMS					
16. SECURITY CLASSIFICATION OF:			17. LIMITATION OF ABSTRACT Same as Report (SAR)	18. NUMBER OF PAGES 29	19a. NAME OF RESPONSIBLE PERSON
a. REPORT unclassified	b. ABSTRACT unclassified	c. THIS PAGE unclassified			

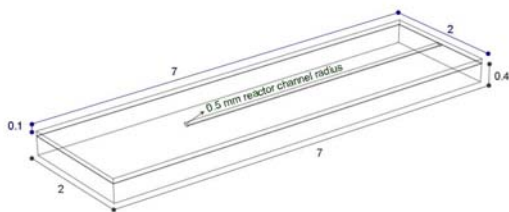


Figure 1. Geometry of microreactor model. All units are given in cm, except for the explicitly labeled reactor channel which is 0.5 mm or 500 μm .

Inside the reactor channel was manganese dioxide (MnO_2), a known H_2O_2 decomposition catalyst⁶. The activation energy and frequency factor, the kinetic parameters that control the reaction rate, were derived from preliminary results of experimental data collected during MnO_2 catalyzed hydrogen peroxide decomposition. The activation energy, E_a , and frequency factor, A , were 20,400 J/mol and 2,910 $\text{mol}/(\text{m}^3\cdot\text{s}\cdot\text{g}_{\text{cat}})$ respectively. These values are similar to those in literature for MnO_2 -catalyzed H_2O_2 decomposition reactions.⁷

The model was sequentially developed first solving mass, energy, and momentum balances independently. Overall balances were solved manually with known inlet conditions and the assumption of full conversion to verify the numerical results from each of the independently solved differential balances. Next, the model was expanded to solve the differential mass and energy balances dependently. Currently, the model is expanding further to include the momentum balance to relate changes in temperature, concentration, and density.

Initially, the model treated the fluid as a single phase liquid system. This preliminary model lacked an extended surface and displayed high temperature rise. To make the single phase model more realistic, a stainless steel extended surface was added and the mass and energy balances were refined. Multiphase considerations via the momentum balance are gradually being introduced into the model. Maintaining the single liquid phase assumption, the momentum was incorporated using the incompressible Navier Stokes equations. Efforts are presently underway to integrate the non-isothermal flow application mode to solve the momentum

balance with variable density as a function of other model parameters.

2.2 Governing Equations and Assumptions

All equation parameters were in SI units. For specific details related to nomenclature and units of all constants and expressions refer to the table entitled Model Parameter Details in the appendix.

Mass Balance. The mass balance of the microreactor system included the diffusion of H_2O_2 into liquid water and H_2O_2 , the bulk flow of the evolving fluid mixture (consisting primarily of liquid H_2O_2 solution in water, and O_2 gas) down the reactor channel, and consumption of H_2O_2 resulting from the decomposition reaction. To model the mass balance, the built-in convection and diffusion application mode in COMSOL was used. Equation 1 governed the convection and diffusion mass balance.

$$\nabla(-D_{\text{eff}}\nabla C) + u_s \cdot \nabla C = r_{\text{H}_2\text{O}_2} \quad (1)$$

In equation 1, D_{eff} gave the diffusivity of H_2O_2 into the liquid water, hydrogen peroxide solution. Due to time constraints the diffusivity term neglected diffusion interactions with the catalyst. The mass balance solved for the variable, concentration, C , the consumed H_2O_2 concentration. The variable u_s represented the superficial velocity of the fluid. The rate of reaction based on the consumption of hydrogen peroxide, $r_{\text{H}_2\text{O}_2}$, was established assuming first order kinetics weighted via an inputted catalyst mass, M_{cat} (equation 2).

$$r_{\text{H}_2\text{O}_2} = -k_{\text{rxn}} C * M_{\text{cat}} \quad (2)$$

The water and oxygen production rates were related to $r_{\text{H}_2\text{O}_2}$ (equations 3 and 4 respectively).

$$r_{\text{H}_2\text{O}} = -r_{\text{H}_2\text{O}_2} \quad (3)$$

$$r_{\text{O}_2} = -0.5 * r_{\text{H}_2\text{O}_2} \quad (4)$$

A conventional Arrhenius relationship with temperature, T , defined the reaction rate constant, k_{rxn} , coupling it to the energy balance (equation 5). The activation energy, E_a , and frequency factor, A , remained as previously defined in the model description.

$$k_{\text{rxn}} = A e^{-E_a / RT} \quad (5)$$

Energy Balance. The energy balance of the microreactor system included conduction, advective input and output due to the feed and exit streams, exothermic heat generation due to reaction, latent heat, and the heat of water vaporization. To model the energy balance, the built-in convection and conduction application mode in COMSOL was used. Equation 6 governed the convection and conduction energy balance.

$$\nabla(-k_{eff}\nabla T) + u_s c_p \rho T = \Delta H_{rxn} * r_{H_2O_2} - LH + \Delta H_{vap} * r_{H_2O} \quad (6)$$

In equation 6, k_{eff} gave the effective thermal conductivity of the reactor channel including the thermal conductivity of catalyst. The energy balance solved for the variable temperature, T , coupling it to the mass balance equation. The term, u_s , still represented the superficial velocity of the liquid. The term c_p represented heat capacity and the term, ρ , the density of the liquid in the microchannel.

The heat of reaction, ΔH_{rxn} , defined the heat released during the exothermic decomposition reaction. The latent heat term, LH , described the contribution of the heat capacities per species required to increase the temperature to the boiling point of water (equation 7).

$$LH = c_{p,H_2O}(373 - T_o) * r_{H_2O} + c_{p,O_2}(373 - T_o) * r_{O_2} \quad (7)$$

The remaining term of the energy balance, ΔH_{vap} , expressed the energy required to vaporize water based on rate of water production during the reaction.

Momentum Balance. To model the momentum balance, the built-in incompressible Navier Stokes application mode in COMSOL was used. Equation 8 (incompressible Navier Stokes) and equation 9 (equation of continuity) governed the incompressible Navier Stokes momentum balance.

$$\rho(\mathbf{U} \cdot \nabla)\mathbf{U} = \nabla \cdot [-p\mathbf{I} + \eta(\nabla\mathbf{U} + (\nabla\mathbf{U})^T)] \quad (8)$$

$$\nabla \cdot (\mathbf{U}) = 0 \quad (9)$$

The density, ρ , was modeled as an average of the liquid and gas comprising the fluid weighted by the mole fractions of H_2O_2 , H_2O , and O_2 species respectively and changed as the reaction progressed (equation 10). This average density

was applied under the assumption that the generated oxygen gas was homogeneously dispersed throughout the liquid solution. The viscosity was given by η . The momentum balance solved for the velocity field, \mathbf{U} , and the pressure, p , using both equations.

$$\rho = y_{H_2O_2}\rho_{H_2O_2s} + y_{H_2O}\rho_{H_2O} + y_{O_2}\rho_{O_2} \quad (10)$$

Although, the simulation results are not available for this paper, models are currently under development using the built-in non-isothermal flow application mode in COMSOL to better account for multiphase effects. The non-isothermal flow application solves the compressible Navier Stokes equations for weakly compressible flows (flows with Mach numbers < 0.3).⁸ Neglecting the effects of the catalyst in the flow channel and using low initial flow rates maintained the conditions defining weakly compressible fluid flow. Equation 11 (compressible Navier Stokes) and equation 12 (equation of continuity with density term) govern the non-isothermal momentum balance.

$$\rho(\mathbf{U} \cdot \nabla)\mathbf{U} = \nabla \cdot [-p\mathbf{I} + \eta(\nabla\mathbf{U} + (\nabla\mathbf{U})^T) - (2\eta/3 - \kappa)(\nabla \cdot \mathbf{U})\mathbf{I}] \quad (11)$$

$$\nabla \cdot (\rho\mathbf{U}) = 0 \quad (12)$$

The density, ρ , remained defined according to equation 10 previously given. The momentum balance solves for the velocity field, \mathbf{U} , and the pressure, p , using both equations. The term, η , represents the fluid viscosity of the solution, whereas κ gave the dilatational viscosity. Using the solved velocity field, the mass and energy balances couple to the momentum balance relating the density and viscosity changes to the concentration and temperature distributions.

2.3 Boundary Conditions

For a tabular synopsis of the current model's boundary conditions and their affiliated equations refer to the table entitled Summary of Boundary Conditions in the appendix.

Mass Balance. The only subdomain active for the mass balance was the reactor microchannel. The inlet boundary condition was initial concentration. The outlet boundary condition was convective flux. Insulation defined the boundary of microchannel walls.

Energy Balance. For all simulations, the energy balance's inlet boundary condition was initial temperature and the outlet boundary condition was convective flux. Initially, the wall boundary was set to a constant temperature to model active cooling. This successfully reduced temperature rise, but remains impractical in physical application. We subsequently set the boundary condition on all external surfaces of the microreactor system to heat flux to simulate convective cooling. Continuity defined the remaining interfacing boundaries.

Momentum Balance. Like, the mass balance, the only active subdomain for the momentum balance was the microchannel. The boundary condition for the inlet was initial superficial velocity. No slip described the boundary condition at the reactor walls. To define the outlet boundary condition normal pressure/normal flow was selected and the pressure value was set to zero.

3. Simulation Results

To obtain a preliminary assessment of cooling capabilities in a H_2O_2 decomposition microreactor, the microchannel was modeled alone under convective cooling. Despite increased surface to volume ratio, approximately $2500 \text{ m}^2/\text{m}^3$ compared to $500 \text{ m}^2/\text{m}^3$ in conventionally sized reactors, the maximum simulated temperature was 385 K and the heat rise was 92 K (Figure 2). Even with the microchannel geometry under convective cooling, the temperature rise was significant. Figure 2 displays the temperature increase, hydrogen peroxide consumption, and oxygen production down the center of the microchannel using an initial volumetric flow rate of $2\text{e}^{-9} \text{ m}^3/\text{s}$ of 50% w/w H_2O_2 for this simulation.

To facilitate convective cooling, the surface area around the microchannel was extended. Simulating liquid phase mass and energy balances in the microreactor model with the extended surface area reduced heat rise considerably to 7 K. The maximum temperature was 300 K (Figure 3). Figure 3 also displays the temperature increase, hydrogen peroxide consumption, and oxygen production using an initial volumetric flow rate of $2\text{e}^{-9} \text{ m}^3/\text{s}$ of 50% w/w H_2O_2 down the center of the microchannel embedded in the extended surface area that was convectively cooled.

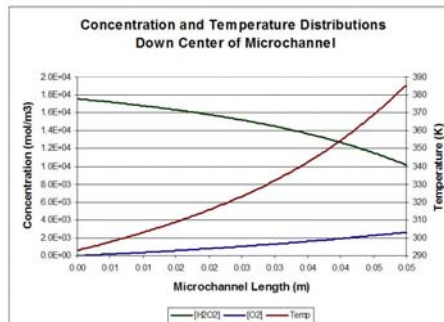


Figure 2. Temperature, and H_2O_2 and O_2 concentration distributions using an initial volumetric flow rate of $2\text{e}^{-9} \text{ m}^3/\text{s}$ of 50% w/w H_2O_2 down the center of the directly convectively cooled microchannel.

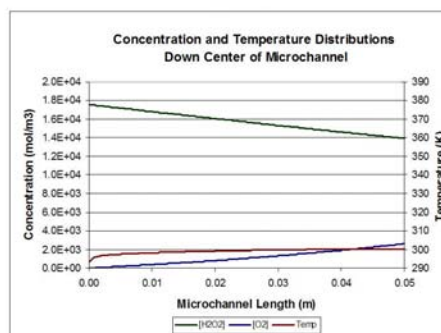


Figure 3. Temperature, and H_2O_2 and O_2 concentration distributions using an initial volumetric flow rate of $2\text{e}^{-9} \text{ m}^3/\text{s}$ of 50% w/w H_2O_2 down the center of the microchannel including the convectively cooled extended surface area.

The extended surface area successfully enabled thermal management with minimal effect on oxygen gas generation.

Beginning the integration of multiphase effects, the momentum balance was introduced. Maintaining the single liquid phase assumption of the previous model, the incompressible Navier Stokes equations were used to solve the flow field of the liquid in the microchannel. As expected for an initial volumetric flow rate $2\text{e}^{-9} \text{ m}^3/\text{s}$ of 50% w/w H_2O_2 the simulated temperature rise was minimal at 7 K (Figure 4). Figure 4 illustrates the thermal distribution across the microreactor unit of this 3D model. The consumed H_2O_2 and O_2 generated concentrations were equivalent to the earlier simulations, indicating modest conversion (Figure 5 and 6).

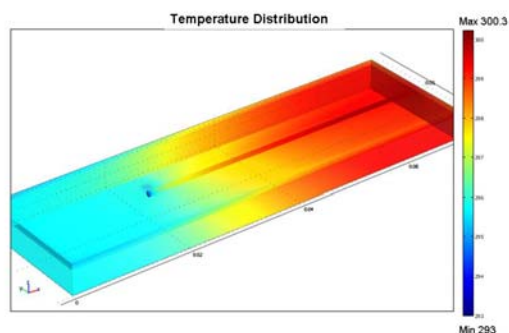


Figure 4. Three dimensional temperature distribution using an initial volumetric flow rate of $2\text{e}^{-9} \text{ m}^3/\text{s}$ of 50% w/w H_2O_2 over the convectively cooled microreactor.

Figures 5 and 6 show the 3D model results for the H_2O_2 and O_2 generated concentrations respectively.

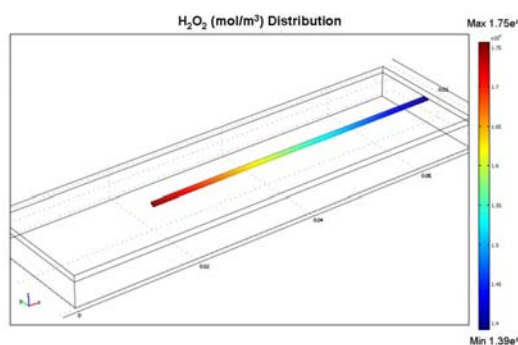


Figure 5. Three dimensional H_2O_2 concentration distribution using an initial volumetric flow rate of $2\text{e}^{-9} \text{ m}^3/\text{s}$ of 50% w/w H_2O_2 over the convectively cooled microreactor.

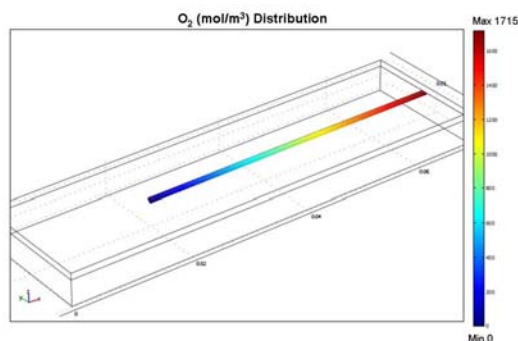


Figure 6. Three dimensional O_2 concentration distribution using an initial volumetric flow rate of $2\text{e}^{-9} \text{ m}^3/\text{s}$ of 50% w/w H_2O_2 over the convectively cooled microreactor.

Models using the non-isothermal application mode for the momentum balance remain under development, since the mesh and solver parameters require further adjustment for model convergence.

4. Summary and Future Work

Increasing the surface-to-volume ratio and correspondingly the mass and heat transfer coefficients via a microchannel reactor enables heat management during catalyzed H_2O_2 decomposition. To investigate the mechanism of thermal management, we modeled a lone microchannel reactor (no extended surface) and neglected multiphase considerations. Significant heat rise across the reaction zone resulted (Figure 2). The surface area around the microchannel was extended, enhancing passive convective cooling capabilities. Although this secondary model continued to neglect multiphase considerations, solving only the mass and energy balances, both oxygen production and thermal management were successfully exhibited (Figures 3).

To integrate the multiphase characteristics of the microchannel fluid, the momentum balance was incorporated and is gradually being modified. The momentum balance was initially solved using the incompressible Navier-Stokes equations, which neglected the flow of generated gas, and achieved temperature and concentration distributions (Figures 4-6) that were equivalent to the earlier models (Figures 2 and 3). The present model continues to demonstrate the promise of thermally controlled hydrogen peroxide decomposition in a microreactor (Figures 4-6).

The compressible Navier-Stokes equations according to the restrictions of the non-isothermal application mode in COMSOL are presently being incorporated into the momentum balance. Assuming the fluid flow is at low mach numbers, and generated oxygen gas is homogeneously dispersed, the simulated microreactor system will be able to account for change in fluid density. Ongoing efforts are underway to update and modify the model to more thoroughly simulate multiphase behaviors. For example, there are plans to model the influence of the catalyst on the diffusivity and flow field applying one of the turbulent flow application modes. A comparison between the

non-isothermal flow application mode and the compressible flow application mode would also offer insight into the validity of weakly compressible flow assumption. In addition to continuing modeling updates, experimental data will be collected for model verification and refinement.

Overall, the modeling results showed that thermally manageable, oxygen generation is viable in a microreactor provided there is adequate external surface area to increase convective cooling. In turn, this controllable source of oxygen production offers a potential means for facilitating air-independent SOFC operation.

5. References

1. UUV Master Plan, **Sec. 4.2.1**, pp. 60-61 (2004)
2. Besser, R., Microchemical Systems for UUV/AUV Power Systems Presentation, (2004)
3. Papadaki, M.; Marques-Domingo, E.; Gao, J.; and Mahmud, T.P., *Journal of Loss Prevention in Process Industrie*, **06** 024 (2005)
4. Davis, N.S.; Keefe, J.H., *Industrial and Engineering Chemistry*, **48** 4 (1956)
5. Ehrfeld, W.; Volker H.; Holger, L., *Microreactors: New Technology for Modern Chemistry*, 1st ed.; pp. 5-8. WILEY-VCH, Weinheim, (2000)
6. Hasan, M.A.; Zaki, M. I.; Pasupulety, L.; Kumari, K.; *Applied Catalysis*, **181** pp. 171–179 (1999)
7. Deraz, N. M.; Salim, H.H.; El-Aal, A.A., *Materials Letters*, **53** pp. 102–109 (2002)
8. COMSOL, Questions and Answers from the Support Desk, *COMSOL News*, p.17 (2007)

6. Acknowledgements

The authors gratefully acknowledge the funding and resources for this research provided by the Office of Naval Research University Laboratory Initiative. We would also like to acknowledge COMSOL technical support for their aid throughout the ongoing development of this model.

7. Appendices

Table 1: Model Parameter Details			
Constants			
Equation Symbol	COMSOL assignment	Value	Description (SI units)
	vfo	2.00E-09	Initial Volumetric Flow Rate (m ³ /s)
	To	293	Initial Temperature (K)
	caoww	50	Initial H ₂ O ₂ % w/w Concentration
	yao	0.346	Initial Mole Fraction H ₂ O ₂
	ybo	0.654	Initial Mole Fraction H ₂ O
	rhoa	1195	Initial Fluid Density (kg/m ³)
$\rho_{H_2O_2}$	rha	1097	Average H ₂ O ₂ Density (0-50% w/w) solution (kg/m ³)
ρ_{H_2O}	rhb	998	Density of Water (kg/m ³)
ρ_{O_2}	rhc	1.3	Average Oxygen Density between 273 and 350 K (kg/m ³)
k_{eff}	keff	5.65	Effective Thermal Conductivity of Reactor Microchannel (W/m ² K)
	sigmac	3.93E-07	Cross Sectional Area of Microchannel (m ²)
	Tambient	290	Ambient Temperature (K)
	hconv	10	Estimated Natural Convective Heat Flux for Air (W/m ² *K)
	cao	17564	Initial H ₂ O ₂ Reactant Concentration (mol/m ³)
	mwa	0.034	Molecular Weight of H ₂ O ₂ (kg/mol)
	mwb	0.018	Molecular Weight of H ₂ O (kg/mol)
ΔH_{rxn}	deltaH	98200	Heat of Reaction (J/mol)
E_a	aE	2.04E+04	Activation Energy with MnO ₂ decomposition catalyst (J/mol)
A	Af	2911	Frequency Factor for Rate Constant (mol/(m ³ *s*gcatal))
R	Rg	8.314	Ideal Gas Constant (J/(mol*K))
	radius	0.0005	Microchannel Radius (m)
	cpa	3731	Average H ₂ O ₂ (0-50%w/w) solution heat capacity(J/kg*K)
M_{cat}	Mcat	0.03	Mass of Catalyst (g)
	Deffhh2o	7.85E-10	Average effective diffusivity of H ₂ O ₂ into water (m ² /s)
	Deffhh	2.71E-12	Average effective diffusivity of H ₂ O ₂ into H ₂ O ₂ (m ² /s)
	rhoss	8000	Density of Stainless Steel 316 (kg/m ³)
	cpss	500	Heat Capacity of Stainless Steel 316 (J/kg*K)
	Kss	16.3	Thermal Conductivity of Stainless Steel 316 (W/(m*K))
cp_{H_2O}	cpb	75.43	Heat Capacity of Water (J/mol*K)
cp_{O_2}	cpc	29.39	Heat Capacity of Oxygen (J/mol*K)
	Po	1.01E+05	Initial Pressure at Inlet (Pa)
	dvis	1.15E-03	Average dynamic viscosity of 0-50% w/w H ₂ O ₂ solution (Pa*s)
	cco	0	Initial concentration of oxygen (mol/m ³)

Scalar Expressions			
Equation Symbol	COMSOL assignment	Expression	Description (SI units)
	us	vfo/sigmac	Initial Superficial Velocity of Fluid (m/s)
k_{rxn}	krxn	$A \cdot \exp((-aE/(Rg \cdot T)))$	Reaction Rate Constant as a Function of Temperature (mol/(m ³ s ³ gcat))
r_{H2O2}	rt	-krxn*Mcat*c	Rate Law for Elementary 1st Order Irreversible Reaction (mol/(s*m ³))
r_{H2O}	rtb	-rt	Rate Law for Elementary 1st Order Irreversible Reaction; Water Production (mol/(s*m ³))
r_{O2}	rtc	0.5*rtb	Rate Law for Elementary 1st Order Irreversible Reaction; Oxygen Production (mol/(s*m ³))
	Xconv	(cao-c)/cao	Conversion
C_{O2}	co2	$cao \cdot (0.5 \cdot X_{conv}) / (1 + 0.5 \cdot y_{ao} \cdot X_{conv}) \cdot (T_o/T)$	Concentration of Oxygen Generated (mol/m ³) assuming negligible pressure change
C_{H2O}	ch2o	$cao \cdot ((y_{bo}/y_{ao}) + X_{conv})$	Concentration of water (mol/m ³) assuming negligible pressure change
y_{H2O2}	yh2o2	$c/(c+co2+ch2o)$	Mole fraction of H ₂ O ₂
y_{H2O}	yh2o	$co2/(c+co2+ch2o)$	Mole fraction of H ₂ O
y_{O2}	yo2	$ch2o/(c+co2+ch2o)$	Mole fraction of O ₂
LH	hnipc	$cpb \cdot (373 - T_o) \cdot rtb + cpc \cdot (373 - T_o) \cdot rtc$	Latent Heat (Heat Needed to Initiate Phase Change) (W/m ³)
ΔH_{vap}	deltaV	-49.004*T + 58754	Heat of Water Vaporization as a Function of Temperature (Heat Needed to Vaporize Water) (J/mol)
D_{eff}		$Deff_{hh} \cdot y_{H2O2} + Deff_{hh2o} \cdot y_{H2O}$	Diffusion of H ₂ O ₂ into Liquid Solution (m ² /s)
ρ	rhom	$c/(c+co2) \cdot rha + co2/(c+co2) \cdot rhc$	Average Density of H ₂ O ₂ solution and Oxygen Gas Mixture (Kg/m ³)

Table 2: Summary of Boundary Conditions		
Mass Balance		
Boundary	Boundary Condition Assigned in COMSOL	COMSOL equation
Inlet	Concentration	$C = c_o = c_{ao}$
Outlet	Convective Flux	$\mathbf{n} \cdot (-D_{eff} \nabla C) = 0 \quad \dagger$
Reactor Walls	Insulation / Symmetry	$\mathbf{n} \cdot (-D_{eff} \nabla C + C \mathbf{u}_s) = 0$
Energy Balance		
Inlet	Temperature	$T = T_o$
Outlet	Convective flux	$\mathbf{n} \cdot (-k_{eff} \nabla T) = 0$
Interfaces	Continuity	$\mathbf{n} \cdot (\mathbf{q}_1 - \mathbf{q}_2) = 0;$ $\mathbf{q}_i = -k_{eff,i} \nabla T_i + \rho_i c_{p,i} \mathbf{u}_i T_i$
External Surfaces	Heat Flux	$\mathbf{n} \cdot (-k_{eff} \nabla T + \rho c_p \mathbf{u} T) = h_{conv} \cdot (T - T_{ambient})$
Momentum Balance		
Inlet	Inflow / Outflow Velocity	$\mathbf{U} = \langle \mathbf{u}_o, 0, 0 \rangle$
Outlet	Normal Flow/Pressure	$P = 0$
Reactor Walls	No Slip	$\mathbf{U} = 0$
$\dagger \mathbf{n}$ represent the outward normal vector		

Modeling Controlled Hydrogen Peroxide (H_2O_2) Decomposition for a SOFC Oxidant Source in a Microreactor



(Example xz Reactor Temperature Profile)

COMSOL Users Conference: October 5, 2007

Elizabeth Lennon:

Stevens Institute of Technology Hoboken, NJ

Dr. A. Alan Burke:

Naval Undersea Warfare Center Newport, RI

Dr. Ronald Besser:

Stevens Institute of Technology Hoboken, NJ



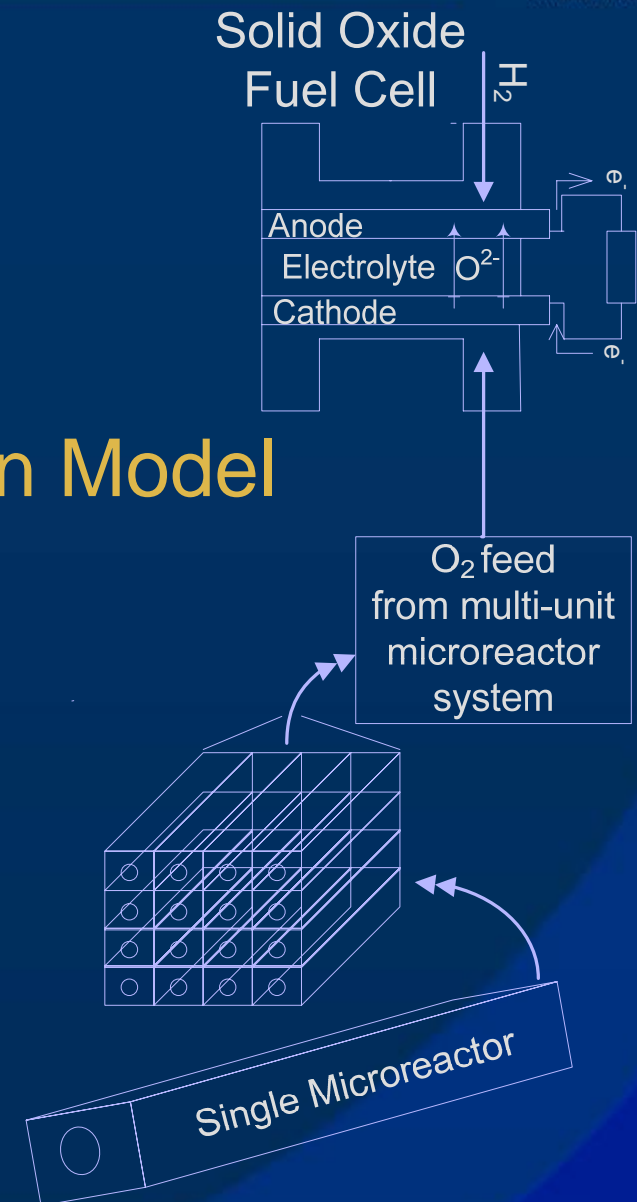
Overview

I. Motivation & Objectives

II. Initial H_2O_2 Decomposition Model

III. Current Model

IV. Future Model Refinement



Motivation

H₂O₂ decomposition



Dense Oxygen Source

(0.0215 moles O₂/ml in 50% liquid H₂O₂)

vs

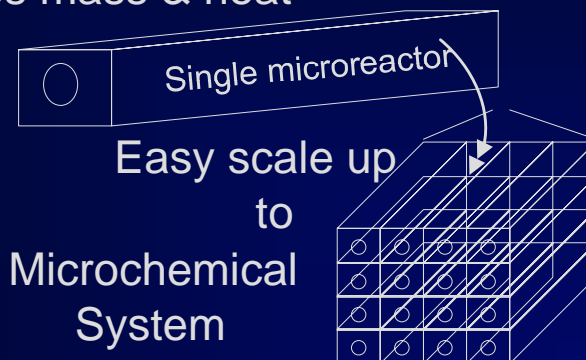
0.035 moles O₂/ml in solid NaClO)

$$\Delta H_{\text{rxn}} = -98.2 \text{ kJ/mol}$$

Highly exothermic reaction

Microreactor Features:

4040 m²/m³ > conventional 10² m²/m³
improves mass & heat transfer



UUVs:
Lack efficient,
air-independent
power sources



UUV
Example

Fuel cells:
High endurance energy supply; but
**need oxidant in air-independent
environment**

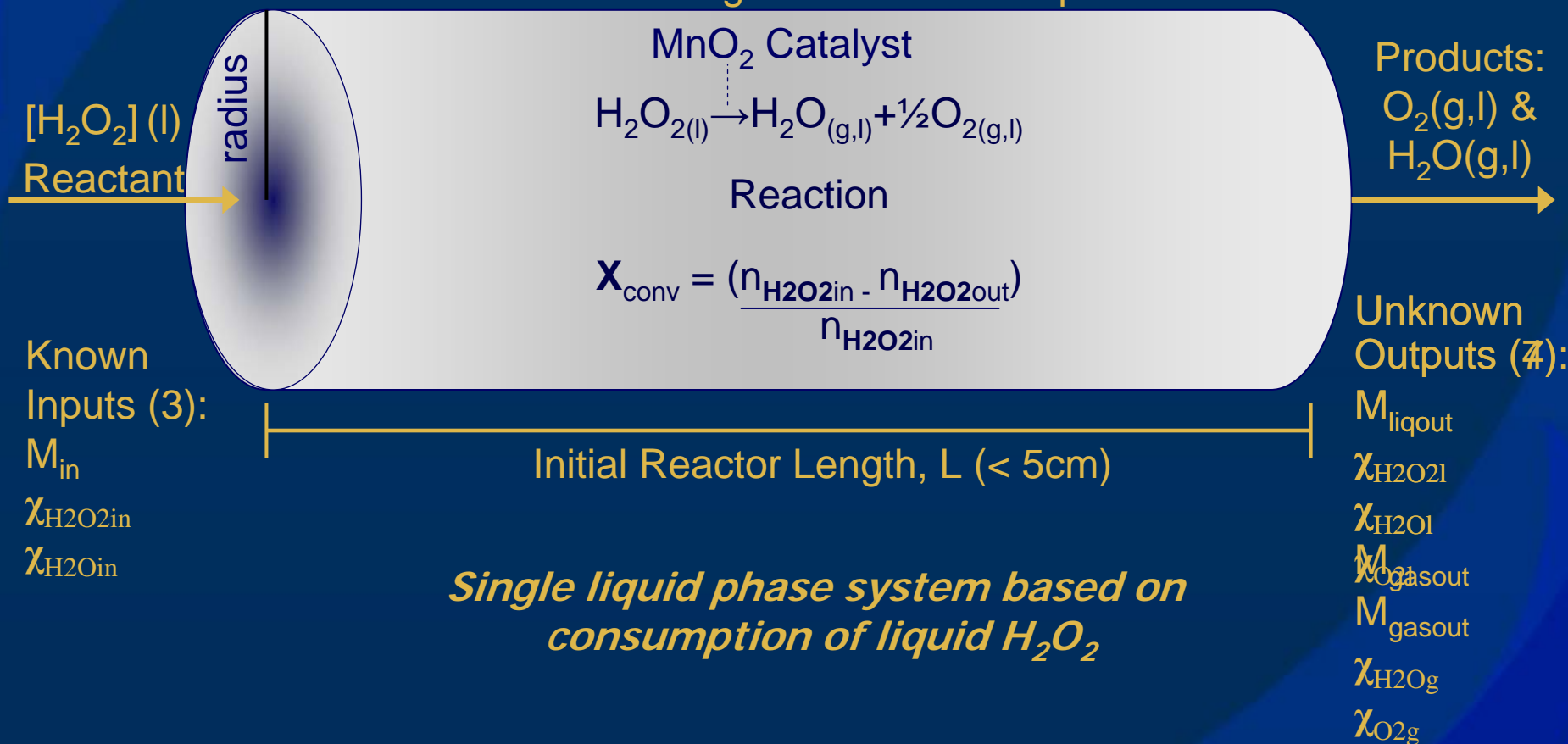
Major Modeling Objectives

- ★ Display temperature control
- ★ Determine max [H₂O₂] for controlled decomposition

Initial H₂O₂ Decomposition Reactor Model

Description & Assumptions

Wall Boundary Condition:
Convective Cooling or Constant Temperature



Steady State Analysis with Stated COMSOL Application Modes Governing Equations (all Units in SI)

Mass Balance: Convection and Diffusion

[H₂O₂] (variable)

$$\nabla(-D_{H_2O_2eff} \nabla C_{H_2O_2}) + U_s \cdot \nabla C_{H_2O_2} = r_{H_2O_2}$$

Average Diffusivity
Liquid Solution
(constant)

Superficial
Velocity
(constant)

1st order rate of reaction

$$r_{H_2O_2} = -k_{rxn} C_{H_2O_2} * M_{cat}$$

Rate Constant
(F(T))

Catalyst
Mass
(constant)

Energy Balance: Convection and Conduction

Temperature
(variable)

Average
Density
(constant)

Heat of
Reaction
(constant)

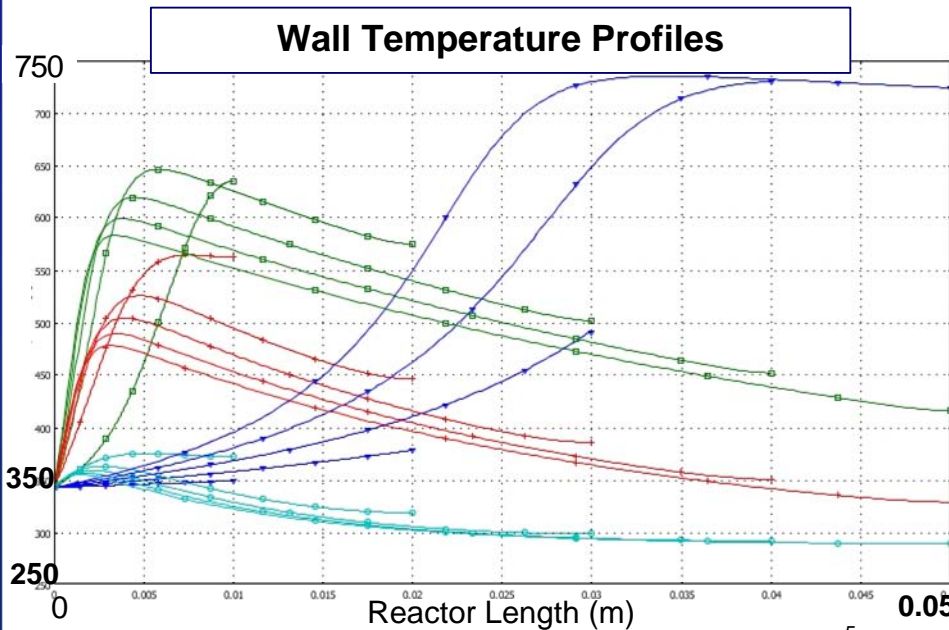
$$\nabla(-k_{eff} \nabla T) + U_s c_p \rho \nabla T = \Delta H_{rxn} * r_{H_2O_2}$$

Effective Thermal
Conductivity of Material
in Microchannel (constant)

Average Heat Capacity
of Fluid in Micro-
channel (constant)

Initial H_2O_2 Decomposition Reactor Model

Simulation Findings (Initially 50% weight H_2O_2 concentration for all runs)



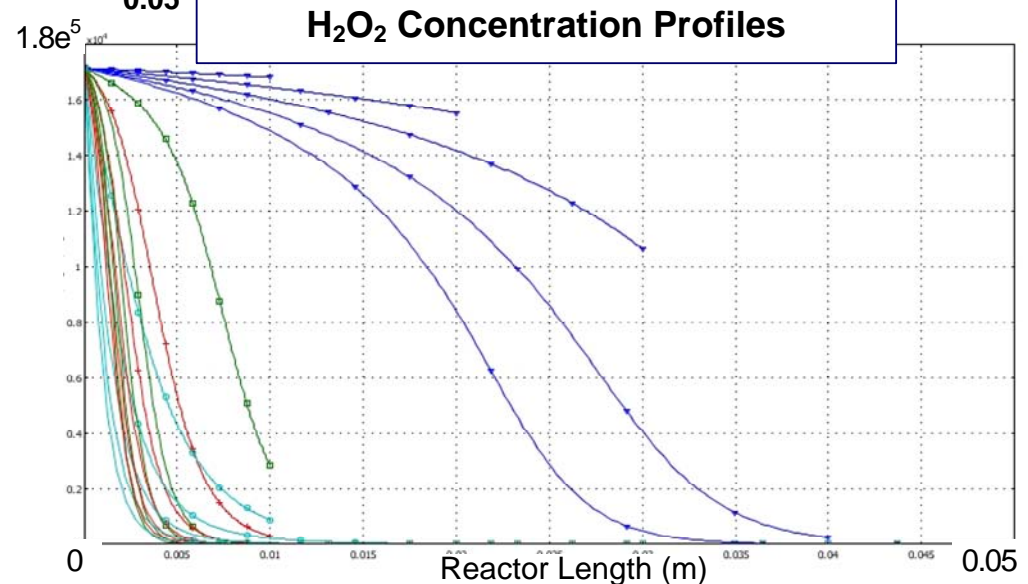
Volumetric Flow Rates (m^3/s):
2e-9, 2e-10, 1e-10, 2e-11

Conclusion:

- Heat rise occurs due to heat generated from reaction, even under convective cooling.
- Need additional cooling mechanism

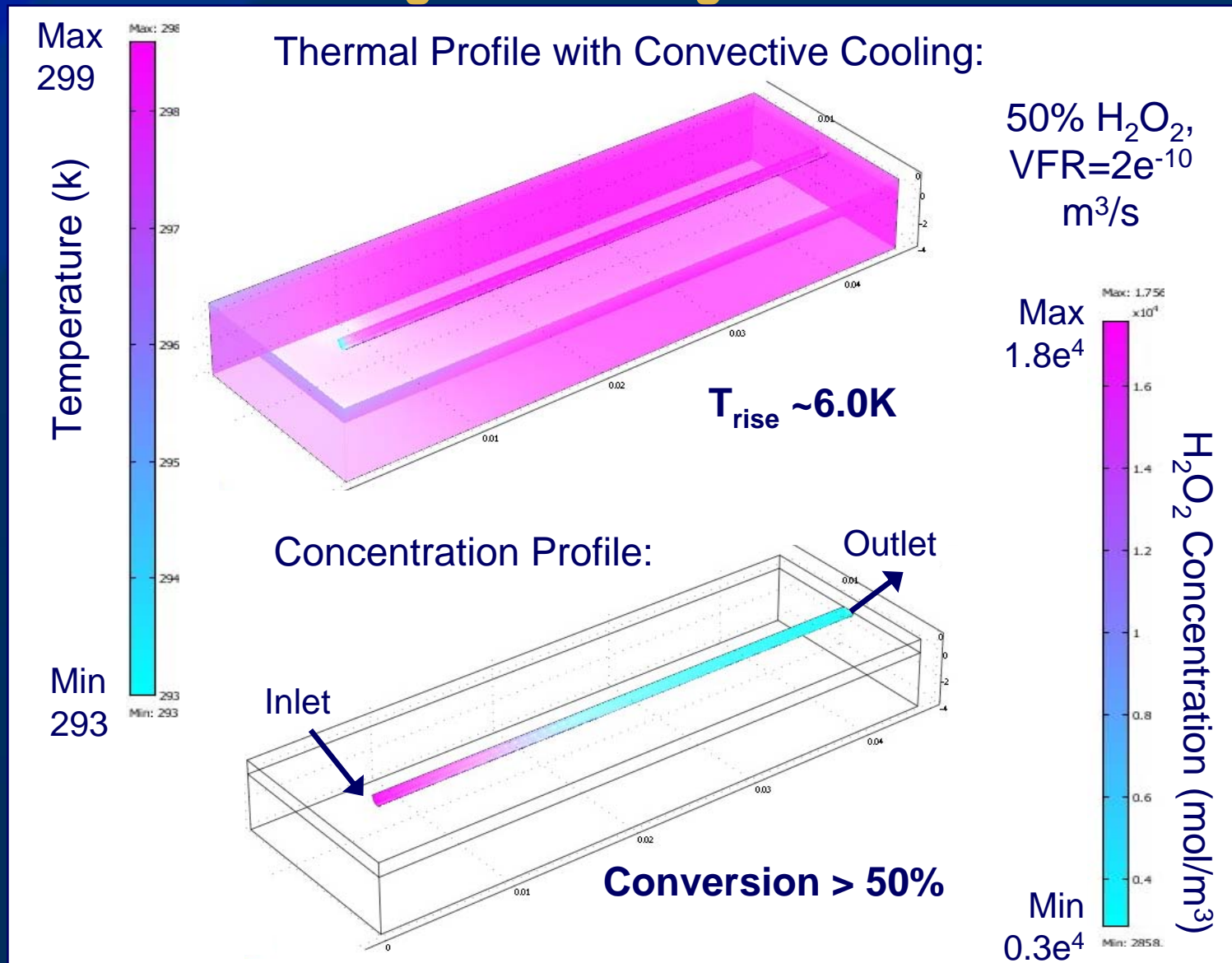
Conclusion:

- Conversion of reactant effectively 100% for reactor lengths greater than 0.04 m for illustrated volumetric flow rates.



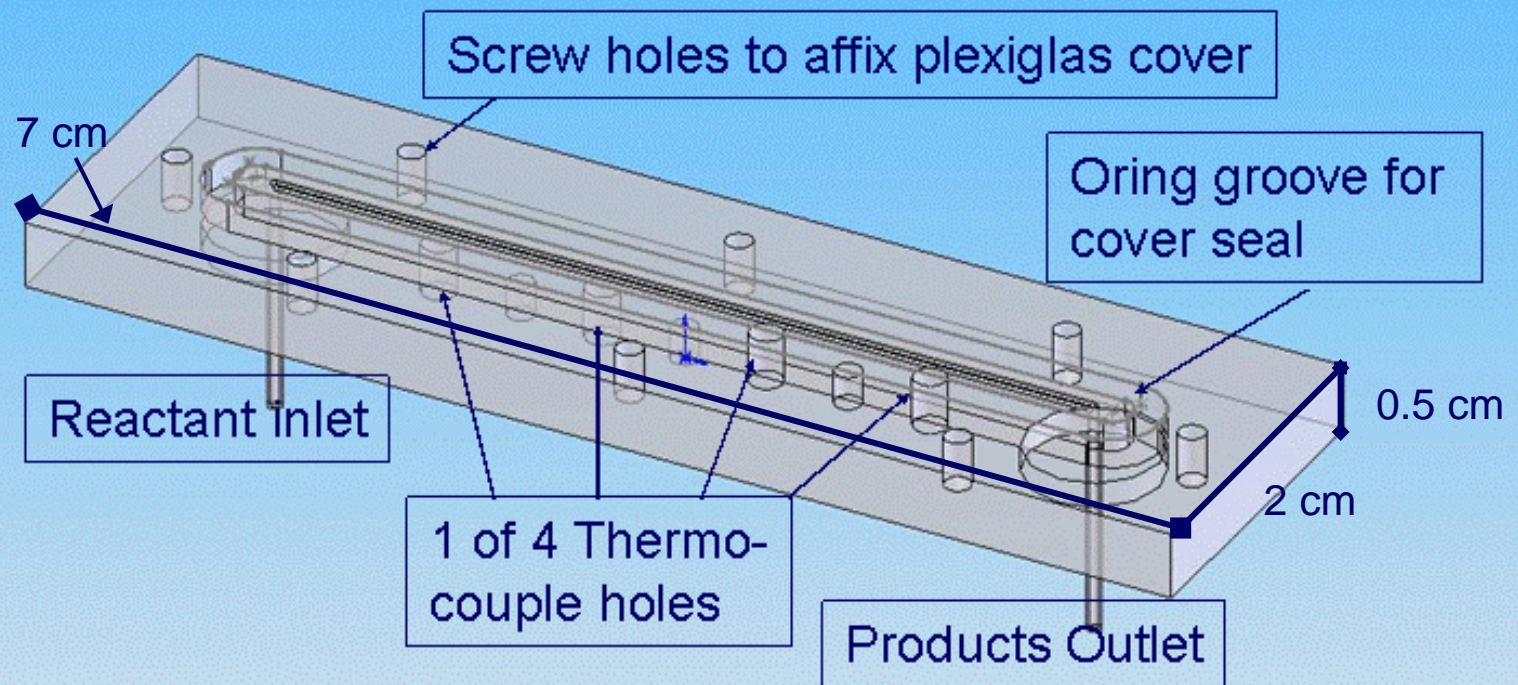
Initial H_2O_2 Decomposition Reactor Model

Simulation Findings: Extending the Surface Area



Initial H_2O_2 Decomposition Reactor Model

Basis for Experimental Reactor and Present Model



Note – reactor is sealed with a plexiglas cover for imaging abilities

Steady state analysis using Stated COMSOL Application Modes

Mass Balance (MB): Convection and Diffusion

$$\nabla \left(-\mathbf{D}_{\text{H}_2\text{O}_2\text{eff}} \nabla \mathbf{C}_{\text{H}_2\text{O}_2} \right) + \mathbf{u}_s \cdot \nabla \mathbf{C}_{\text{H}_2\text{O}_2} = r_{\text{H}_2\text{O}_2}$$

Energy Balance (EB): Convection and Conduction

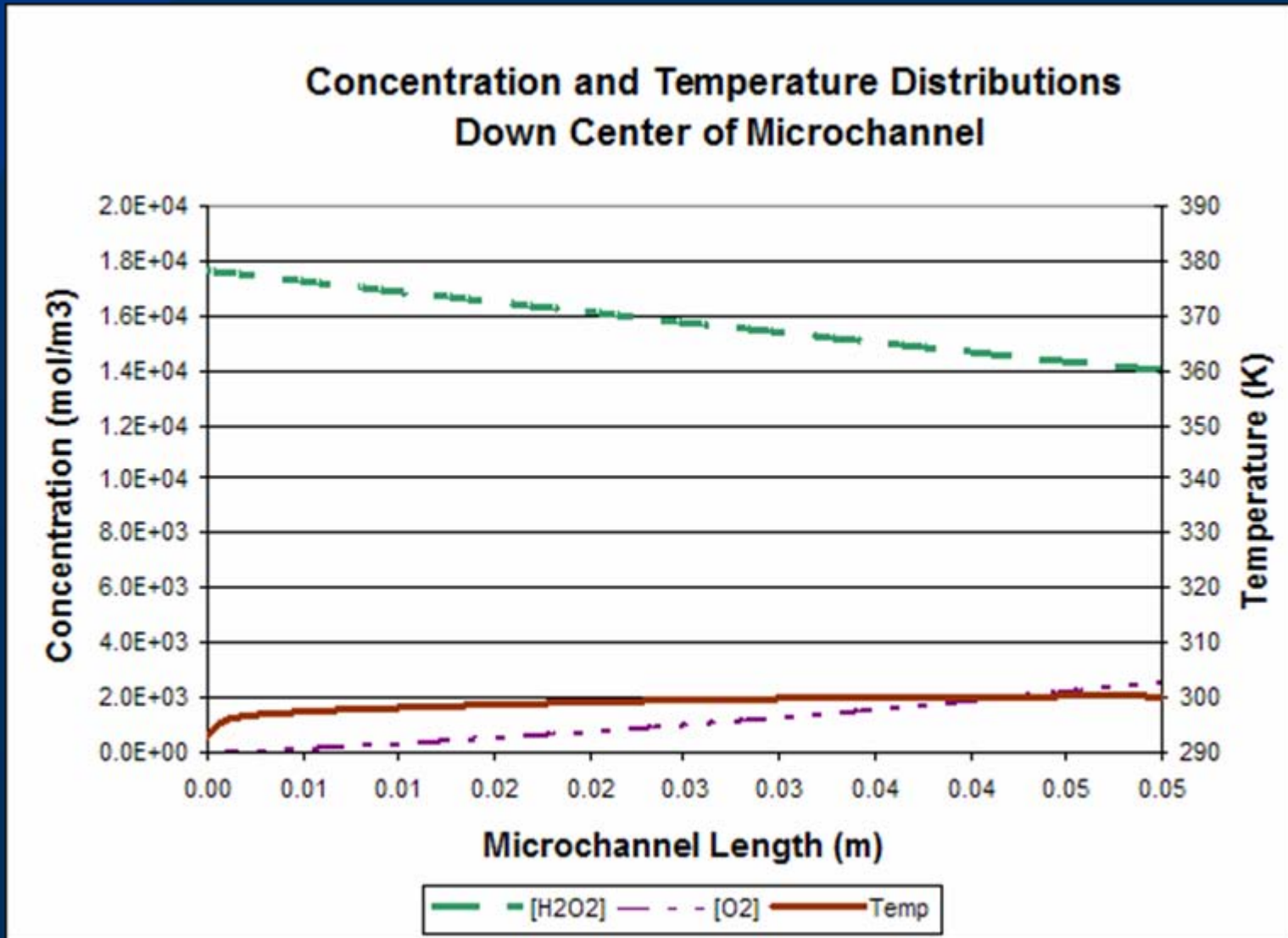
$$\nabla \left(-k_{\text{eff}} \nabla \mathbf{T} \right) + \mathbf{u}_s c_p \rho \nabla \mathbf{T} = \Delta H_{\text{rxn}} * r_{\text{H}_2\text{O}_2} - \mathbf{SH} + \Delta H_{\text{vap}} * r_{\text{H}_2\text{O}}$$

Momentum Balance (MoB) 3.3: Nonisothermal Flow

$$\rho(\mathbf{U} \cdot \nabla) \mathbf{U} = \nabla \cdot [-p\mathbf{I} + \eta(\nabla \mathbf{U} + (\nabla \mathbf{U})^T) - (2\eta/3 - \kappa)(\nabla \cdot \mathbf{U})\mathbf{I}]$$

$$\nabla \cdot (\rho \mathbf{U}) = 0$$

Intermediate Model Findings (version 3.2)

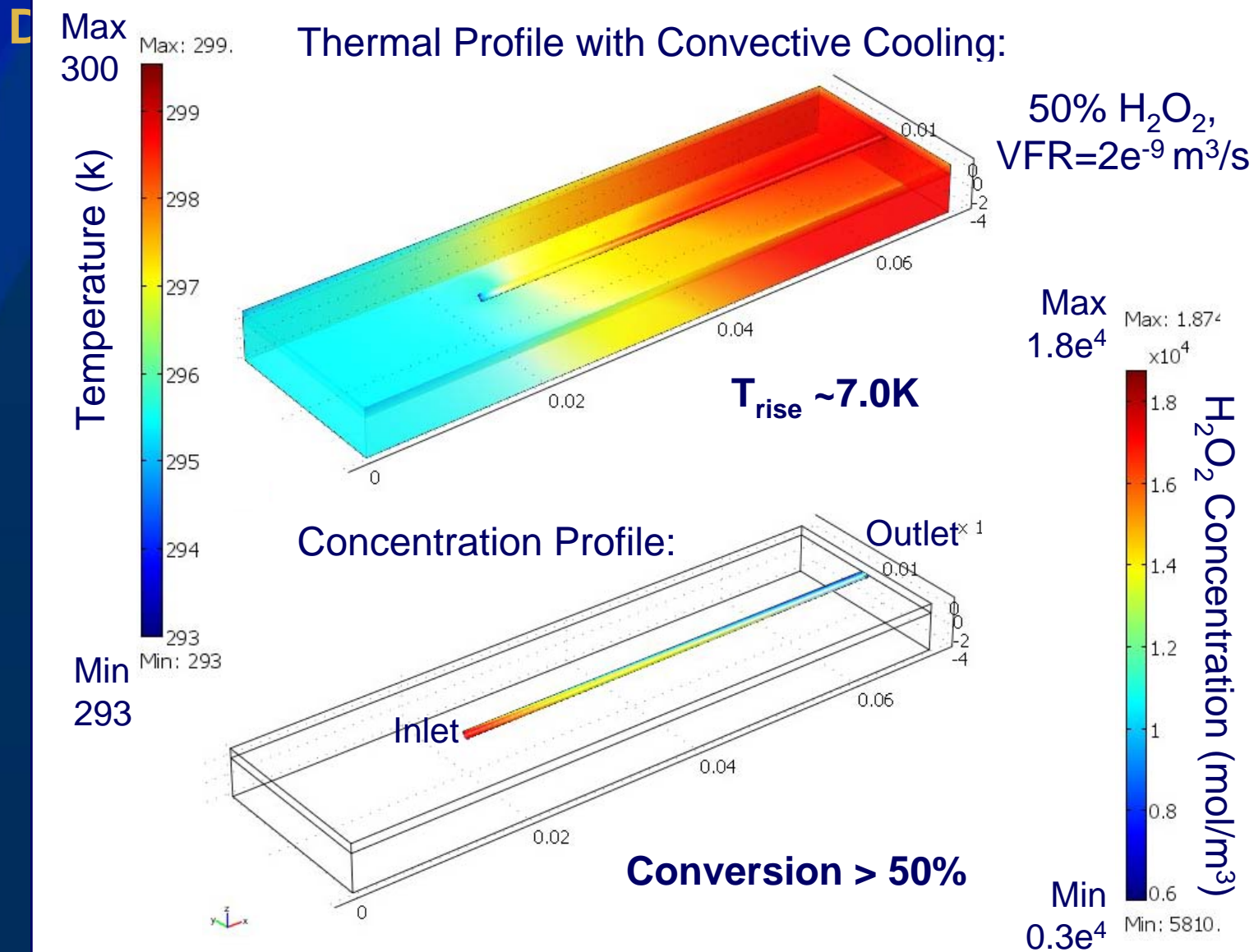


Numerical Verification (all Units in SI)

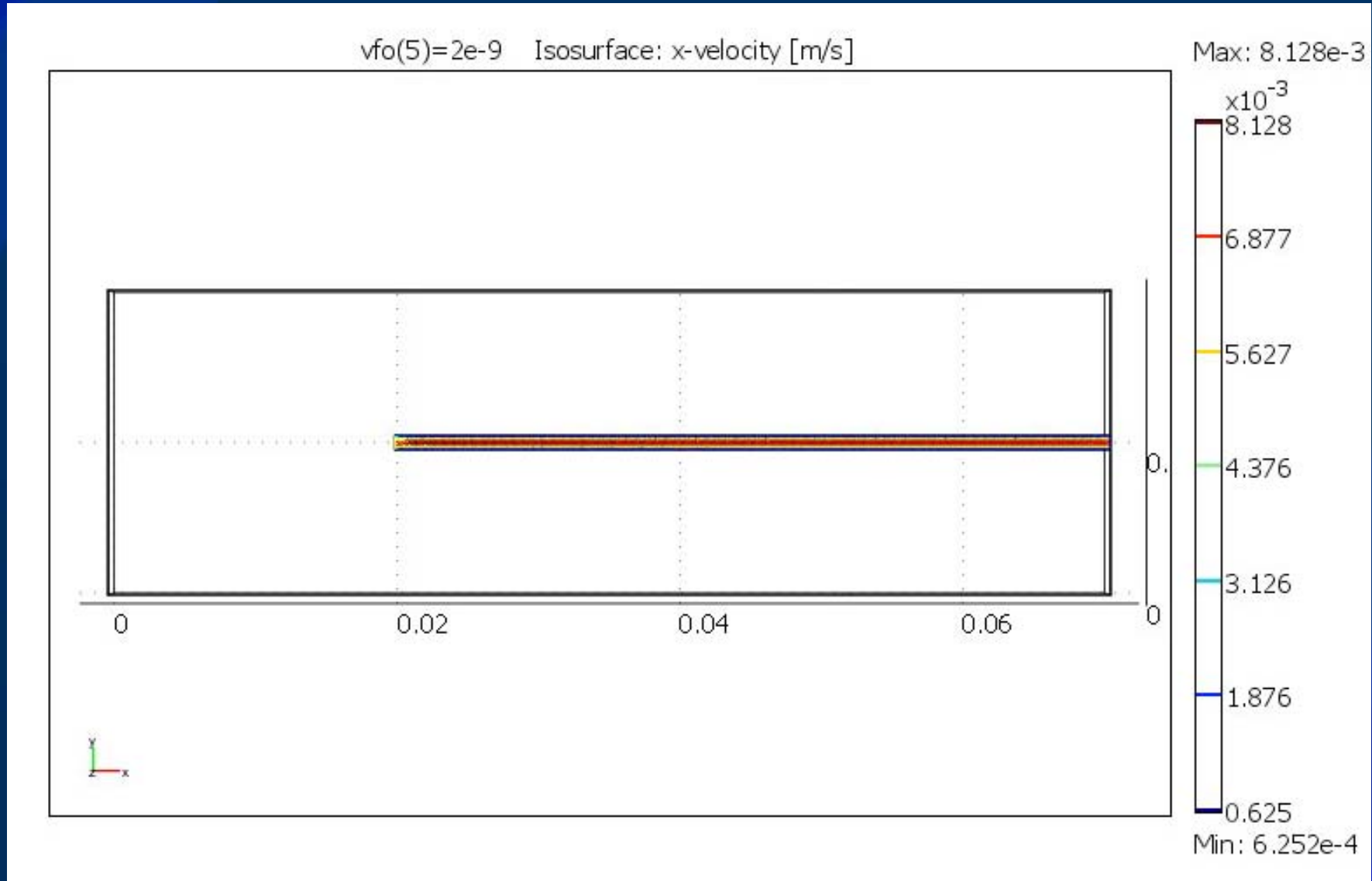
	<i>Initial Volumetric Flow Rate ($\text{e}^{-9} \text{m}^3/\text{s}$)</i>					
<i>Balance</i>	20. 0	8.3 0	5.0 0	2.7 0	2.0 0	0.8 3
% Nonclosure Energy Balance	17	11	6	2	6	18
% Nonclosure Mass Balance	27	10	6	3	2	0
% Difference Reynolds #	17	17	17	16	15	13

Current Microreactor Model

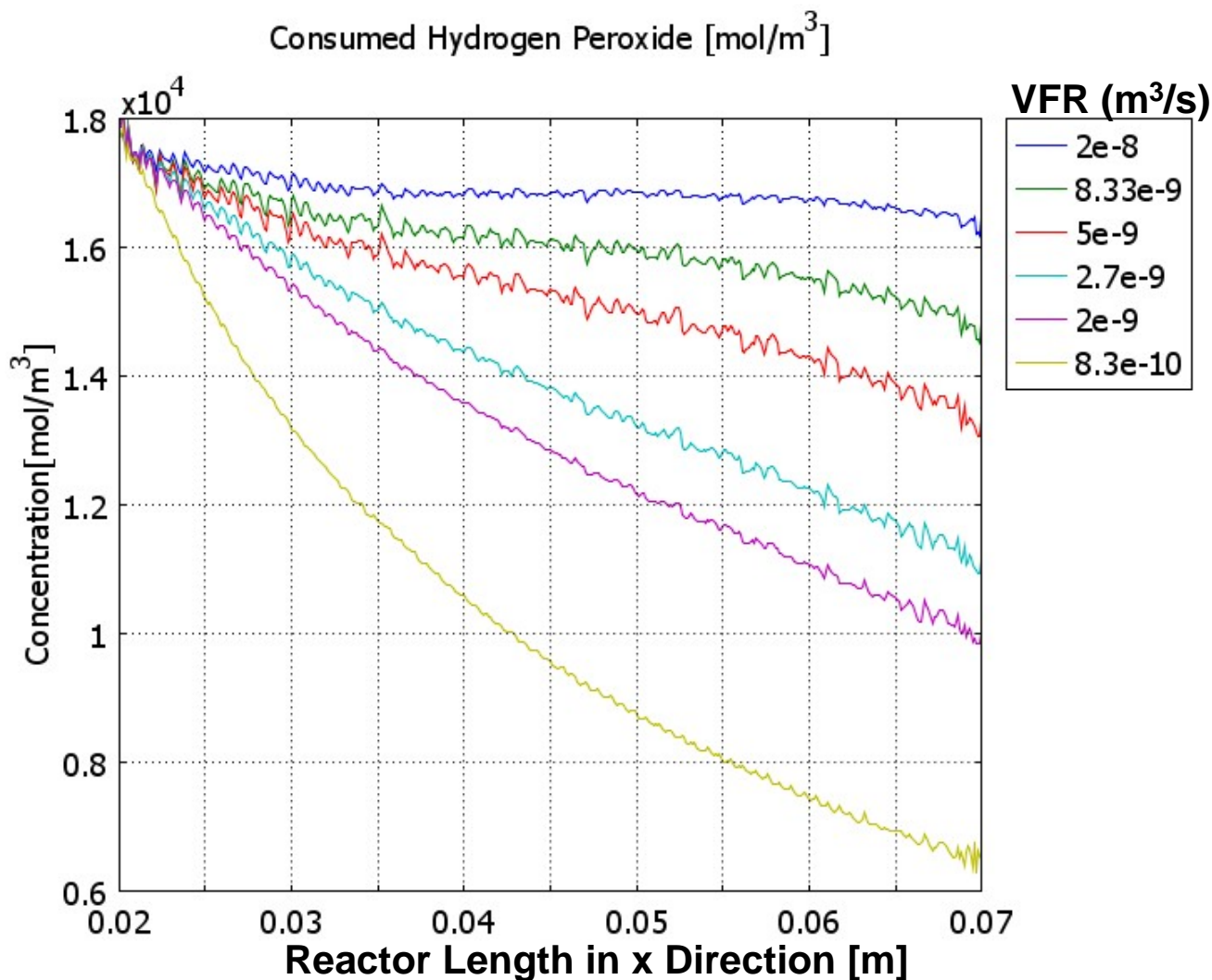
Simulation Findings: Temp / $C_{H_2O_2}$



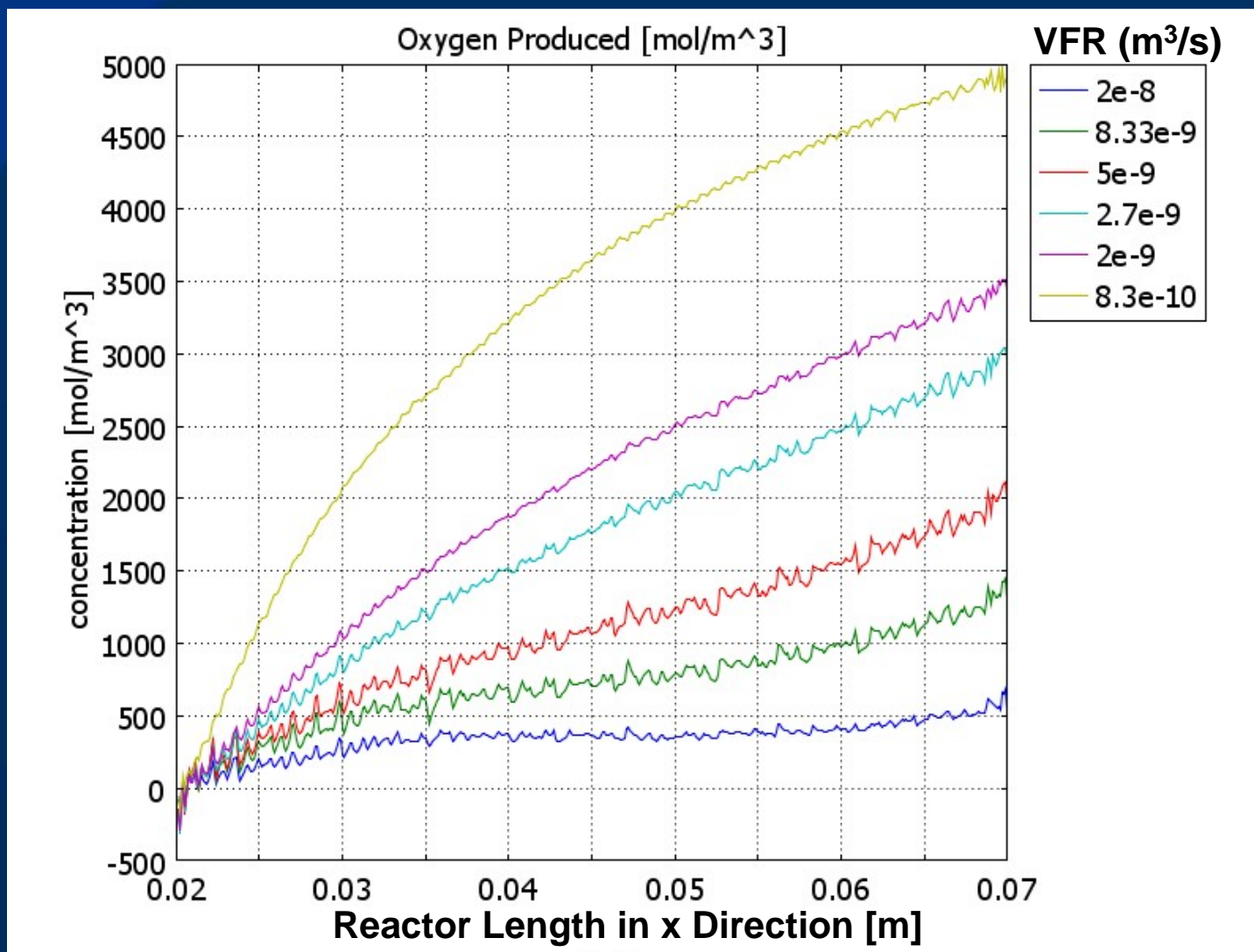
Simulation Findings: X Direction Velocity (m/s)



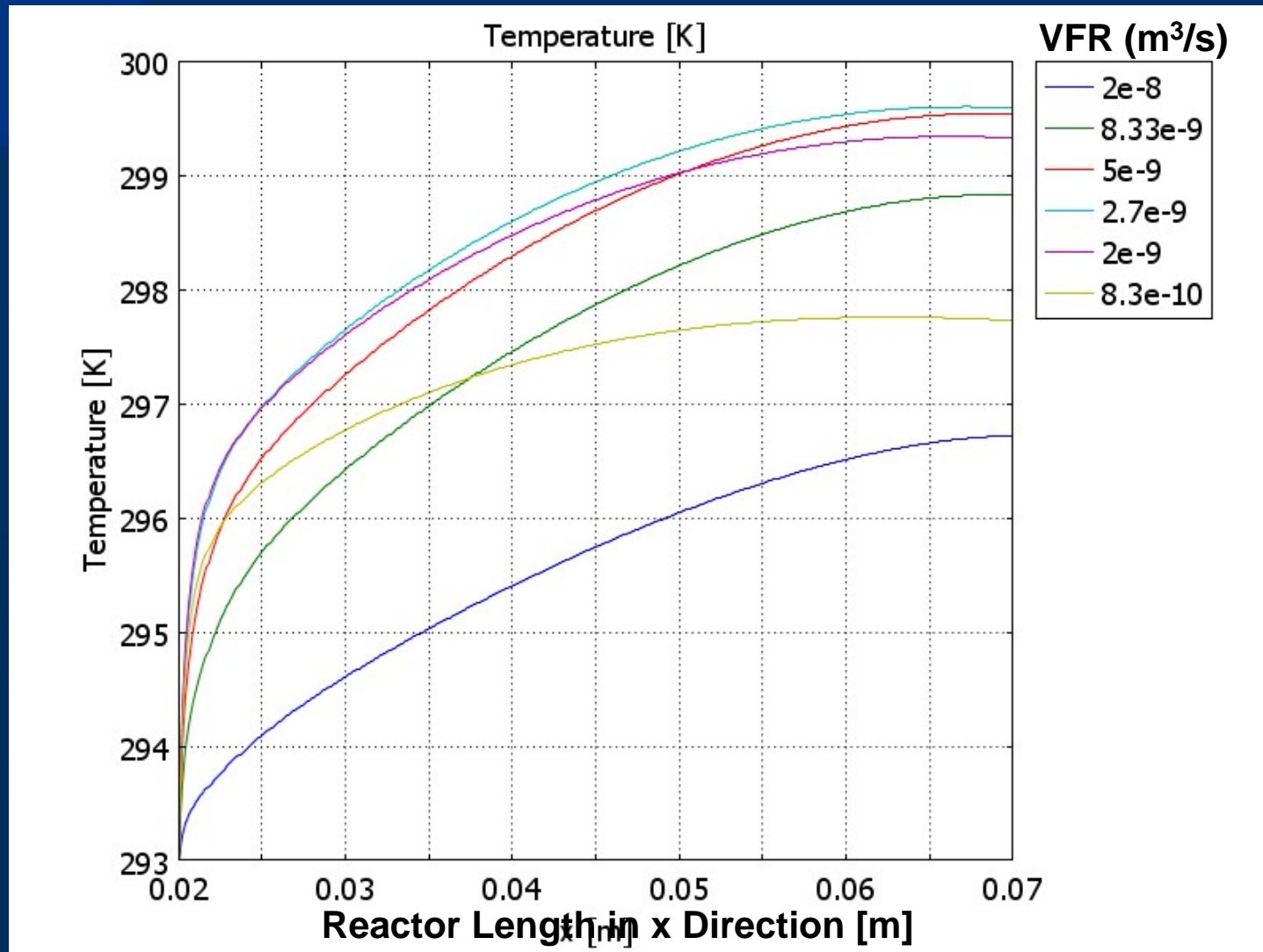
Simulation Findings: Hydrogen Peroxide Consumption



Simulation Findings: Oxygen Gas Generation



Simulation Findings: Temperature Rise



Simulations and O₂ Required for UUV

Ex. For 2.5 kW UUV Power Output Need 0.6 moles O₂ /min

With 20 cm tube for 100% conversion of
8.3e⁻¹⁰ m³/s flow w/ [H₂O₂]_{in} = 1.8e⁴ mol/m³

O₂ gen./tube = 4.48e⁻⁴ mol/min

tubes for 2.5 kW_{system} = 1300

Reactor Volume =

1300 tubes (0.16 cm³/tube) = 200 cm³

A 0.5 Liter space would likely be enough for
this reactor with cooling components

Future Model Refinement

- Improve solver parameters to minimize artifacts on concentration profiles
- Continue integrating multiphase considerations
 - Different types of flow (ie slug flow)
 - Bubble generation from O₂ gas
- Compare experimental data to be collected for continued model refinement

Acknowledgments

Thank you

Dr. R. S. Besser

Dr. A. A. Burke

Funding agencies ONR, ULI, ASEE, NREIP

S.I.T. CBME and Physics Faculty and

Researchers, particularly Dr. P. Corrigan, Dr. E. Whittaker, Dr. B. Gallois, and Dr. D. M. Kalyon

COMSOL support

Backup Slide 1

Table 1: Model Parameter Details

Constants			
Equation Symbol	COMSOL assignment	Value	Description (SI units)
	vfo	2.00E-09	Initial Volumetric Flow Rate (m ³ /s)
	To	293	Initial Temperature (K)
	caoww	50	Initial H ₂ O ₂ % w/w Concentration
	yao	0.346	Initial Mole Fraction H ₂ O ₂
	ybo	0.654	Initial Mole Fraction H ₂ O
	rhoa	1195	Initial Fluid Density (kg/m ³)
$\rho_{H_2O_2s}$	rha	1097	Average H ₂ O ₂ Density (0-50% w/w) solution (kg/m ³)
ρ_{H_2O}	rhb	998	Density of Water (kg/m ³)
ρ_{O_2}	rhc	1.3	Average Oxygen Density between 273 and 350 K (kg/m ³)
k_{eff}	keff	5.65	Effective Thermal Conductivity of Reactor Microchannel (W/m ² *K)
	sigmac	3.93E-07	Cross Sectional Area of Microchannel (m ²)
	Tambient	290	Ambient Temperature (K)

	hconv	10	Estimated Natural Convective Heat Flux for Air (W/m ² *K)
	cao	17564	Initial H ₂ O ₂ Reactant Concentration (mol/m ³)
	mwa	0.034	Molecular Weight of H ₂ O ₂ (kg/mol)
	mwb	0.018	Molecular Weight of H ₂ O (kg/mol)
ΔH_{rxn}	deltaH	98200	Heat of Reaction (J/mol)
E_a	aE	2.04E+04	Activation Energy with MnO ₂ decomposition catalyst (J/mol)
A	Af	2911	Frequency Factor for Rate Constant (mol/(m ³ *s*(gcat)))
R	Rg	8.314	Ideal Gas Constant (J/(mol*K))
	radius	0.0005	Microchannel Radius (m)
	cpa	3731	Average H ₂ O ₂ (0-50%w/w) solution heat capacity(J/kg*K)
M_{cat}	Mcat	0.03	Mass of Catalyst (g)
	Deffhh2o	7.85E-10	Average effective diffusivity of H ₂ O ₂ into water (m ² /s)

Backup Slide 2

	Deffhh	2.71E-12	Average effective diffusivity of H ₂ O ₂ into H ₂ O ₂ (m ² /s)
	rhoss	8000	Density of Stainless Steel 316 (kg/m ³)
	cpss	500	Heat Capacity of Stainless Steel 316 (J/kg*K)
	Kss	16.3	Thermal Conductivity of Stainless Steel 316 (W/(m*K))
cp_{H_2O}	cpb	75.43	Heat Capacity of Water (J/mol*K)
cp_{O_2}	cpc	29.39	Heat Capacity of Oxygen (J/mol*K)
	Po	1.01E+05	Initial Pressure at Inlet (Pa)
	dvis	1.15E-03	Average dynamic viscosity of 0-50% w/w H ₂ O ₂ solution (Pa*s)
	cco	0	Initial concentration of oxygen (mol/m ³)

Scalar Expressions			
Equation Symbol	COMSOL assignment	Expression	Description (SI units)
	us	vfo/sigmac	Initial Superficial Velocity of Fluid (m/s)
k_{rxn}	krxn	$Af \cdot \exp((-aE/(Rg \cdot T)))$	Reaction Rate Constant as a Function of Temperature (mol/(m ³ *s*gcatal))
$r_{H_2O_2}$	rt	$-krxn \cdot Mcat \cdot c$	Rate Law for Elementary 1st Order Irreversible Reaction (mol/(s*m ³))
r_{H_2O}	rtb	-rt	Rate Law for Elementary 1st Order Irreversible Reaction; Water Production (mol/(s*m ³))
r_{O_2}	rtc	$0.5 \cdot rtb$	Rate Law for Elementary 1st Order Irreversible Reaction; Oxygen Production (mol/(s*m ³))
	Xconv	$(cao - c)/cao$	Conversion
C_{O_2}	co2	$cao \cdot (0.5 \cdot Xconv) / (1 + 0.5 \cdot yao \cdot Xconv) \cdot (To/T)$	Concentration of Oxygen Generated (mol/m ³) assuming negligible pressure change
C_{H_2O}	ch2o	$cao \cdot ((ybo/yao) + Xconv)$	Concentration of water (mol/m ³) assuming negligible pressure change

Backup Slide 3

$y_{H_2O_2}$	$y_{H_2O_2}$	$c/(c+c_{O_2}+c_{H_2O})$	Mole fraction of H_2O_2
y_{H_2O}	y_{H_2O}	$c_{O_2}/(c+c_{O_2}+c_{H_2O})$	Mole fraction of H_2O
y_{O_2}	y_{O_2}	$c_{H_2O}/(c+c_{O_2}+c_{H_2O})$	Mole fraction of O_2
LH	hnipc	$cpb*(373-T_o)+cpc*(373-T_o)*rtc$	Latent Heat (Heat Needed to Initiate Phase Change) (W/m^3)
ΔH_{vap}	deltaV	$-49.004*T + 58754$	Heat of Water Vaporization as a Function of Temperature (Heat Needed to Vaporize Water) (J/mol)
D_{eff}		$D_{effH_2O_2}*y_{H_2O_2}+D_{effH_2O}*y_{H_2O}$	Diffusion of H_2O_2 into Liquid Solution (m^2/s)
ρ	rhom	$c/(c+c_{O_2})*\rho_{H_2O_2} + c_{O_2}/(c+c_{O_2})*\rho_{H_2O}$	Average Density of H_2O_2 solution and Oxygen Gas Mixture (Kg/m^3)

Table 2: Summary of Boundary Conditions		
Mass Balance		
Boundary	Boundary Condition Assigned in COMSOL	COMSOL equation
Inlet	Concentration	$C=c_{O_2}=c_{H_2O}$
Outlet	Convective Flux	$\mathbf{n} \cdot (-D_{eff} \nabla C) = 0$ †
Reactor Walls	Insulation / Symmetry	$\mathbf{n} \cdot (-D_{eff} \nabla C + C \mathbf{u}) = 0$
Energy Balance		
Inlet	Temperature	$T=T_o$
Outlet	Convective flux	$\mathbf{n} \cdot (-k_{eff} \nabla T) = 0$
Interfaces	Continuity	$\mathbf{n} \cdot (\mathbf{q}_1 - \mathbf{q}_2) = 0;$ $\mathbf{q}_i = -k_{eff,i} \nabla T_i + \rho_i c_{p,i} \mathbf{u}_i T_i$
External Surfaces	Heat Flux	$\mathbf{n} \cdot (-k_{eff} \nabla T + \rho c_p \mathbf{u} T) = h_{conv}*(T - T_{ambient})$
Momentum Balance		
Inlet	Inflow / Outflow Velocity	$\mathbf{U} = \langle u_o, 0, 0 \rangle$
Outlet	Normal Flow/Pressure	$P = P_{atm}$
Reactor Walls	No Slip	$\mathbf{U} = 0$
† \mathbf{n} represent the outward normal vector		